Polyhedron 297 (2026) 118300

Contents lists available at ScienceDirect

Polyhedron

journal homepage: www.elsevier.com/locate/poly

Rhodium complexes of tetradentate tripodal tripyridyl ligands: Phosphate, phosphate monoester, and an unexpected acetimidamide species

Ruojie Huang [a,1], Cameron P. Waghorn [a,1], Timothy D. Christopher [b], Tilo Söhnel [b,c], Tony Chen [a], Allan G. Blackman [a,*]

[a] Department of Chemistry, Auckland University of Technology, Private Bag 92006, Auckland 1142, New Zealand
[b] School of Chemical Sciences, University of Auckland, Auckland 1142, New Zealand
[c] Institute for Advanced Materials and Nanotechnology, Victoria University of Wellington, Wellington 6140, New Zealand

ARTICLE INFO

Keywords:
Rhodium
Cobalt
Tripodal tetraamine ligands
Mass spectrometry
^{31}P NMR spectroscopy

ABSTRACT

The complexes $[Rh(N_4)Cl_2]ClO_4$ (N_4 = tpa, pmea, pmap, tepa) and $[Co(pmea)Cl_2]ClO_4$ have been prepared and characterised (tpa = tris(2-pyridylmethyl)amine, pmea = bis[(2-pyridyl)methyl]-2-[(2-pyridyl)ethyl]amine, pmap = bis[2-(2-pyridyl)ethyl]-(2-pyridylmethyl)amine, and tepa = tris[2-(2-pyridyl)ethyl]amine), and the X-ray crystal structures of $[Rh(pmea)Cl_2]ClO_4$, $[Co(pmea)Cl_2]ClO_4{\cdot}0.61H_2O$, and $[Rh(tepa)Cl_2]ClO_4$ are reported. Reaction of the rhodium complexes with Na_3PO_4 and $Na_2C_6H_5PO_4$ gives chelated phosphate and phenylphosphate complexes for all but the $[Rh(tpa)Cl_2]^+$ starting material, as evidenced by Hi Res Mass Spectrometry and ^{31}P NMR spectroscopy. Reaction of the *in situ*-generated $[Rh(pmap)Cl(MeCN)]^{2+}$ ion with bis(cyclohexylammonium)-t-butylphosphate gives $[Rh(pmap)Cl(N\text{-}cyclohexylacetimidamide)](ClO_4)_2$, which results from attack of cyclohexylamine at the nitrile C atom of coordinated MeCN. The X-ray crystal structure of this complex is reported.

1. Introduction

The complexes of transition metals with phosphate and its derivatives have been a subject of longstanding interest, driven at least in part by the biological importance of inorganic phosphate and phosphate ester species, and their interactions with metal ions in biological systems. [1–7] It is therefore somewhat surprising that only five examples of a transition metal complex containing a chelated phosphate ligand are present in the Cambridge Structural Database (CSD) [8–12]. Similarly, there are only five examples of transition metal complexes containing chelated HPO_4^{2-}, [8,13–15] and, despite the extensive work that has been carried out on the metal-promoted hydrolysis of phosphate esters, there are no examples of a phosphate ester chelated to a transition metal ion. The latter is of particular interest, as it is possible that chelation of a phosphate ester might facilitate nucleophilic attack at the phosphorus atom through both steric (formation of a chelate ring will constrain the bond angles at phosphorus) and electronic (the Lewis acid electron-withdrawing effect of the transition metal ion) effects, and this could be a hitherto unexplored mechanistic pathway for transition metal-promoted phosphate ester hydrolysis. The majority of studies of metal promoted phosphate ester hydrolysis have utilised first row transition metal ions, owing to their rapid rates of ligand exchange that facilitate binding of the phosphate ester and release of the phosphate product. However, this lability can make it difficult to observe important reaction intermediates, and the fact that many of the first row metal complexes that have been used are paramagnetic means that NMR cannot be used either as an aid to identification of species involved in the reaction or as a method for collection of kinetic data. [16] Given that diamagnetic Co(III) complexes, which are nominally substitutionally inert, have been successfully used in many studies of the hydrolysis of phosphate esters, [17–23] we thought that use of even more substitutionally inert starting materials might allow trapping and identification of metal-bound phosphate and phosphate ester species in these reactions. Complexes of Rh(III) are both diamagnetic and more substitutionally inert than those of Co(III), and the Rh(III) chemistry of phosphate and its derivatives has been little studied [24–28]. We therefore chose a series of rhodium complexes containing the tetradentate tripodal tripyridyl ligands shown in Fig. 1 as starting materials for these studies, as

* Corresponding author.
E-mail address: allan.blackman@aut.ac.nz (A.G. Blackman).
[1] Joint first-authors

https://doi.org/10.1016/j.poly.2026.118300
Received 27 May 2026; Accepted 13 July 2026
Available online 14 July 2026

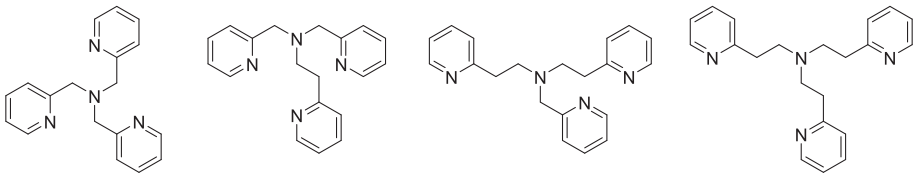

Fig. 1. The tetradentate tripyridyl tripodal ligands used in this study.

complexes of these ligands containing unusual oxoanion chelates such as HCO_3^-, [29,30] HPO_4^{2-}, [13] and HBO_3^{2-} [31] exhibit significant stability. In this paper we report the results of these studies.

2. Experimental

2.1. General

The tetradentate ligands tris(2-pyridylmethyl)amine (tpa), bis[(2-pyridyl)methyl]-2-[(2-pyridyl)ethyl]amine (pmea), bis[2-(2-pyridyl)ethyl]-(2-pyridylmethyl)amine (pmap), and tris[2-(2-pyridyl)ethyl]amine (tepa) were prepared by literature methods. [32,33] $RhCl_3.xH_2O$ was obtained from Precious Metals Online (https://precmet.com.au). The supplier's analysis of this gave Rh = 37.7% by mass, meaning that x = 3.5. X-ray data for $[Rh(pmea)Cl_2]ClO_4$ (CCDC-2555714), $[Rh(tepa)Cl_2]ClO_4$ (CCDC-2555713), and $[Co(pmea)Cl_2]ClO_4.0.61H_2O$ (CCDC-2555715) were collected on a Rigaku Oxford Diffraction XtaLAB-Synergy-S single-crystal diffractometer with a PILATUS 200 K hybrid pixel array detector using Cu Kα radiation (λ = 1.54184 Å), while those for $[Rh(pmap)Cl(L)](ClO_4)_2$ (L = N-cyclohexylacetimidamide) (CCDC-2555712) were collected on a Siemens/Bruker SMART APEX II single-crystal diffractometer with a CCD area detector using graphite-monochromated Mo Kα radiation (λ = 0.71073 Å). The structures were solved by direct methods using either the SHELXS structure solution program [34] or SIR2019, [35] and refined with the SHELXL refinement package [36] using least squares minimization, these programs running within the WinGX [37] or Olex2 [38] software packages. All non-hydrogen atoms were refined anisotropically. Hydrogen atoms were inserted at calculated positions and refined with a riding model or without restrictions. High Resolution Mass spectra were recorded on an Orbitrap Exploris 240 mass spectrometer in positive electrospray ionization (ESI) mode, while Low Resolution spectra were recorded on an Agilent 6420 mass spectrometer. ^{1}H, ^{13}C, ^{31}P, and ^{59}Co NMR spectra were recorded on a Bruker Avance 400 MHz spectrometer, with ^{1}H and ^{13}C chemical shift values (δ) measured relative to residual solvent ([D_6]DMSO) or NaTSP (D_2O), external H_3PO_4 (^{31}P), and external $K_3[Co(CN)_6]$ (^{59}Co).

2.2. Synthesis

2.2.1. Synthesis of $[Rh(tpa)Cl_2]ClO_4$

To a solution of $RhCl_3{\cdot}3.5H_2O$ (0.57 g, 2.1 mmol) in H_2O (20 mL) was added a solution of tpa (0.72 g, 2.5 mmol) in acetonitrile (20 mL). The resulting solution was refluxed for 24 h. After cooling, the dark brown solution was reduced to a low volume (rotavap) and a few drops of concentrated $NaClO_4$(aq) were added, resulting in the precipitation of a yellow brown solid. This was isolated by filtration, washed with ice-cold water (2 × 5 mL), and air-dried. The product was then recrystallised from hot (70 °C) water to afford $[Rh(tpa)Cl_2]ClO_4$ (0.69 g, 58% based on Rh). ^{1}H NMR (D_6-DMSO): δ 9.49 (1H, d), 8.86 (2H, d), 8.09 (2H, td), 7.95 (1H, td), 7.75 (2H, d), 7.61 (3H, m), 7.41 (1H, d), 5.61 (2H, d), 5.32 (2H, s), 5.09 (2H, d). ^{13}C NMR (d^6-DMSO): δ 163.75, 163.12, 151.20, 149.53, 140.83, 140.62, 126.43, 126.08, 125.00, 122.36, 70.76, 70.31. HRMS (ESI): (*m/z*) calcd for $RhC_{18}H_{18}N_4Cl_2^+$: 462.9960 $[M]^+$; found: 462.9959.

2.2.2. Synthesis of $[Co(pmea)Cl_2]ClO_4.H_2O$

To solid $[Co(pmea)O_2CO)]ClO_4$ [29] (1.128 g, 2.158 mmol) in an evaporating basin was added HCl(aq) (6 mol L^{-1}, 45 mL) and the solution was heated on a steam bath for 2 h, over which time the colour changed from orange/red to green and the volume decreased to ~10 mL. To this solution was added a small amount of $NaClO_4$(s) and propan-2-ol (5 mL), and crystalline blue $[Co(pmea)Cl_2]ClO_4.H_2O$ (0.762 g, 66%) was obtained on standing in the refrigerator overnight. ^{1}H NMR (d^6-DMSO): δ 9.77 (1H, dd), 9.15 (d, 1H), 9.08 (d, 1H), 8.12 (td, 1H), 8.02 (td, 1H), 7.91 (td, 1H), 7.80 (d, 1H), 7.58 (m, 2H), 7.46 (m, 3H), 5.49 (d, 1H), 4.80 (d, 1H), 4.48 (m, 2H), 3.72 (dd, 1H), 3.50 (t, 1H), 3.03 (m, 2H). ^{13}C NMR (D_6-DMSO): δ 163.96, 161.55, 159.02, 156.3, 154.36, 151.14, 140.30, 140.10, 139.17, 126.20, 125.55, 124.36, 122.81, 122.65, 120.23, 69.72, 67.60, 55.92, 32.92. ^{59}Co NMR (D_6-DMSO): δ 9748 ppm. HRMS (ESI): (*m/z*) calcd for $CoC_{19}H_{20}N_4Cl_2^+$: 433.0390 $[M]^+$; found: 433.0388.

2.2.3. Synthesis of $[Rh(pmea)Cl_2]ClO_4$

To a solution of $RhCl_3{\cdot}3.5H_2O$ (0.52 g, 1.9 mmol) in H_2O (20 mL) was added a solution of pmea (0.76 g, 2.5 mmol) in acetonitrile (20 mL). The resulting solution was refluxed for 24 h. After cooling, the dark brown solution was reduced to a low volume (rotavap), and a few drops of concentrated $NaClO_4$(aq) were added, giving a yellow brown solid. This was isolated by filtration, washed with ice-cold water (2 × 5 mL) and air-dried. Recrystallisation from hot (70 °C) water gave the desired product (0.62 g, 56% based on Rh). ^{1}H NMR (d^6-DMSO): 9.77 (1H, d), 9.24 (2H, t), 8.17 (1H, t), 8.01 (2H, m), 7.90 (1H, d), 7.64 (2H, m), 7.54 (2H, m), 5.47 (1H, d), 4.91 (2H, m), 4.65 (1H, d), 3.80 (1H, dd), 3.69 (1H, t), 3.44 (2H, m (overlapped by solvent peak)), 3.14 (1H, m). ^{13}C NMR (d^6-DMSO): 163.64, 160.57, 158.95, 155.68, 153.31, 150.54, 141.03, 140.50, 127.95, 126.47, 126.02, 124.61, 124.38, 122.02, 70.68, 68.40, 58.59, 35.23. HRMS (ESI): (*m/z*) calcd for $RhC_{19}H_{20}N_4Cl_2^+$: 477.0110 $[M]^+$; found: 477.0115.

2.2.4. Synthesis of $[Rh(pmap)Cl_2]ClO_4$

To a solution of $RhCl_3{\cdot}3.5H_2O$ (0.51 g, 1.9 mmol) in H_2O (20 mL) was added a solution of pmap (0.77 g, 2.4 mmol) in acetonitrile (20 mL), and the resulting solution was refluxed for 24 h. After cooling, the dark brown solution was reduced to a low volume (rotavap). Addition of a few drops of concentrated $NaClO_4$(aq) resulted in precipitation of a yellow brown solid. This was isolated by filtration, washed with ice-cold water (2 × 5 mL) and air-dried. Recrystallisation from hot (70 °C) water gave the desired product (0.35 g, 31% based on Rh). ^{1}H NMR (d^6-DMSO): δ 9.40 (2H, t), 9.25 (3H, s), 8.04 (6H, m), 7.80 (3H, m), 7.62 (4H, d), 7.51 (3H, d), 7.45 (4H, m), 5.61 (1H, d), 4.70 (1H, d), 4.36 (3H, br t), 3.98 (4H, s), 3.59 (4H, br s), 2.92 (4H, br q). ^{13}C NMR (d^6-DMSO): δ 161.37, 160.65, 154.87, 150.27, 141.33, 140.92, 140.76, 127.93, 127.58, 127.52, 126.13, 124.79, 124.48, 124.11, 123.84, 69.26, 57.66, 34.47, 33.56, 22.98. HRMS (ESI): (*m/z*) calcd for $RhC_{20}H_{22}N_4Cl_2^+$: 491.0270 $[M]^+$; found: 491.0274.

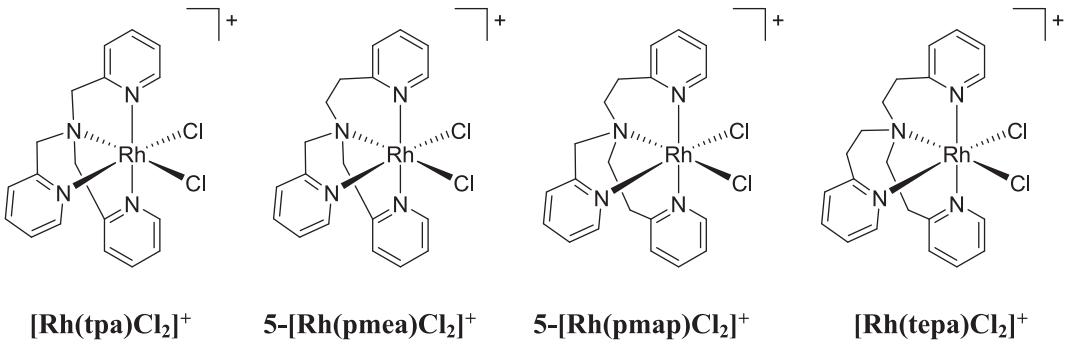

Fig. 2. Structures of the $[Rh(N_4)Cl_2]^+$ cations.

2.2.5. Synthesis of [Rh(tepa)Cl$_2$]ClO$_4$

To a solution of $RhCl_3{\cdot}3.5H_2O$ (0.53 g, 1.9 mmol) in H_2O (20 mL) was added a solution of tepa (0.78 g, 2.3 mmol) in acetonitrile (20 mL) and the resulting solution was refluxed for 24 h. After cooling, the dark brown solution was reduced to low volume (rotavap), and a few drops of concentrated $NaClO_4$(aq) were added, resulting in precipitation of a yellow brown solid. This was isolated by filtration, washed with ice-cold water (2 × 5 mL) and air-dried. Recrystallisation from hot (70 °C) water afforded the desired product (0.67 g, 58% based on Rh). ^{1}H NMR (d^6-DMSO): δ 9.17 (2H, d), 8.57 (1H, d), 8.05 (3H, m), 7.58 (3H, t), 7.51 (1H, t), 7.44 (2H, t), 3.83 (2H, m), 3.66 (2H, m), 3.17 (2H, t), 3.08 (4H, m), 2.50 (2H, m). ^{13}C NMR (d^6-DMSO): δ 162.15, 160.48, 156.48, 154.48, 141.41, 140.50, 127.92, 127.35, 125.22, 123.43, 61.48, 55.95, 35.73, 33.53. HRMS (ESI): (*m/z*) calcd for $RhC_{21}H_{24}N_4Cl_2^+$: 505.0430 $[M]^+$; found: 505.0427.

2.2.6. Synthesis of [Rh(pmap)Cl(L)](ClO$_4$)$_2$ (L = N-cyclohexylacetimidamide)

$[Rh(pmap)Cl_2]ClO_4$ (107.2 mg, 0.18 mmol) and $AgCF_3SO_3$ (53.4 mg, 0.21 mmol) were dissolved in acetonitrile (15 mL). The resulting solution was refluxed for 1 h until a white precipitate formed and the mixture was then filtered through celite. Bis(cyclohexylammonium) t-butylphosphate (56.7 mg, 0.17 mmol) was added to the yellow solution, which was then refluxed for 1 h. The resulting dark yellow solution was filtered (celite) and reduced to dryness (rotavap). The residue was dissolved in water and a concentrated solution of $NaClO_4$ (aq) was added, resulting in the precipitation of a dark yellow solid. This was removed by filtration and washed with ice cold ethanol. Recrystallisation from the minimum volume of hot water gave $[Rh(pmap)Cl(L)](ClO_4)_2$ as X-ray quality yellow crystals. LRMS(ESI): (*m/z*) calcd for $RhC_{28}H_{38}N_6Cl^+$: 596.19 $[M]^+$; found: 596.20.

2.2.7. Reactions of [Rh(N$_4$)Cl$_2$]ClO$_4$ complexes with Na$_3$PO$_4$ and Na$_2$C$_6$H$_5$PO$_4$

The reactions of the rhodium complexes with a two-fold excess of a phosphate species were carried out on small scales (generally 50–100 mg of the rhodium complex) in aqueous solution. The reaction mixtures were heated at 80 °C overnight and hot filtered, and the filtrate was analysed by mass spectrometry. The filtrate was then reduced to dryness and the NMR spectra of the resulting solid materials were recorded.

3. Results and discussion

3.1. Syntheses and characterisation of the [M(N$_4$)Cl$_2$]ClO$_4$ (M =Co, Rh) complexes

The Rh(III) complexes $[Rh(N_4)Cl_2]ClO_4$ (N_4 = tpa, pmea, pmap, tepa) were prepared from the reaction of $RhCl_3{\cdot}3.5H_2O$ with the tetraamine ligand in acetonitrile/water, followed by precipitation with $NaClO_4$ and recrystallisation of the resulting solid from hot water, and their structures are shown in Fig. 2.

Colbran and coworkers have prepared $[Rh(tpa)Cl_2]Cl{\cdot}H_2O$ and $[Rh(pmea)Cl_2]PF_6{\cdot}0.5H_2O$ previously from the reaction of $RhCl_3{\cdot}xH_2O$ with the N_4 ligand in refluxing ethanol. [39] The mass spectra of the rhodium complexes in water (Figs. S1, S3-S5), with the exception of that of $[Rh(tepa)Cl_2]ClO_4$, show only a single major peak, and were all consistent with their proposed formulation as monomeric monocationic species containing two chlorido ligands; the 1+ charge on the cations is confirmed by the *m/z* peak spacing and the presence of two chlorido ligands is consistent with the moderately intense (~60–70%) peak observed at ~2 *m/z* units greater than the base peak in all cases. The mass spectrum of $[Rh(tepa)Cl_2]ClO_4$ shows intense peaks at *m/z* = 505.0427, corresponding to the $[Rh(tepa)Cl_2]^+$ ion (calcd *m/z* = 505.0430) and *m/z* = 487.0766, consistent with the $[Rh(tepa)Cl(OH)]^+$ ion (calcd *m/z* = 487.0770). However, the ^{1}H and ^{13}C NMR spectra of this complex in D_6-DMSO show peaks for only a single species, suggesting that the $[Rh(tepa)Cl(OH)]^+$ ion is formed by hydrolysis of $[Rh(tepa)Cl_2]^+$ in the mass spectrometer. The Co(III) complex $[Co(pmea)Cl_2]ClO_4$ was prepared by reaction of $[Co(pmea)O_2CO)]ClO_4$ [29] with HCl(aq) on a steam bath, and crystallisation following addition of propan-2-ol. The mass spectrum of the blue product (Fig. S2) shows the base peak at *m/z* = 433.0388, which corresponds to the $[Co(pmea)Cl_2]^+$ ion (calcd *m/z* = 433.0390). Lower intensity peaks at *m/z* = 415.0726 and *m/z* = 398.0699 can be assigned to $[Co(pmea)(OH)Cl]^+$ and $[Co(pmea)Cl]^+$ (calcd *m/z* = 415.0730 and 398.0700, respectively). Again, these appear to be formed in the mass spectrometer as the ^{1}H and ^{13}C NMR spectra of $[Co(pmea)Cl_2]ClO_4$ in D_6-DMSO are consistent with only a single species. The ^{59}Co NMR chemical shift of 9748 ppm is significantly greater than that of the $[Co(pmea)O_2CO]^+$ starting material (8509 ppm) [29], attesting to the weaker ligand field exerted by two monodentate chlorido ligands compared to a single chelated carbonato ligand. While $[Rh(pmea)Cl_2]^+$ and $[Co(pmea)Cl_2]^+$ differ only in the identity of the metal ion and are structurally very similar (see below), the much lower lability of the rhodium complex is demonstrated by the fact that it can be recrystallised from 70 °C water without change, while the blue cobalt complex hydrolyses relatively rapidly (minutes) in water at room temperature to give a purple product, presumably $[Co(pmea)(OH_2)Cl]^{2+}$.

The ^{1}H and ^{13}C NMR spectra of the $[Rh(N_4)Cl_2]ClO_4$ complexes in D_6-DMSO (Figs. S16-S25, the complexes have limited water solubility), together with the COSY, HSQC, and HMBC spectra, were consistent with the formulae of the cations being $[Rh(N_4)Cl_2]^+$ in all cases. As has been seen before in 6-coordinate complexes of these N_4 ligands, [29] geometric isomers are possible for both the $[Rh(pmea)Cl_2]^+$ and $[Rh(pmap)Cl_2]^+$ complex cations; the chlorido ligands can lie in the same plane as either a 5-membered, or 6-membered chelate ring of the N_4 ligand, to give the 5- and 6-isomers, respectively. The ^{13}C NMR spectrum of each complex was used to determine which isomer was present. The observation of 4 peaks in the aliphatic region for the $[Rh(pmea)Cl_2]^+$ cation is consistent with the 5-isomer, as is the appearance of 14 peaks in the aromatic region (15 should be observed for the 5-isomer, but the peak at 141.03 ppm is due to two coincident carbon atoms, as confirmed by the

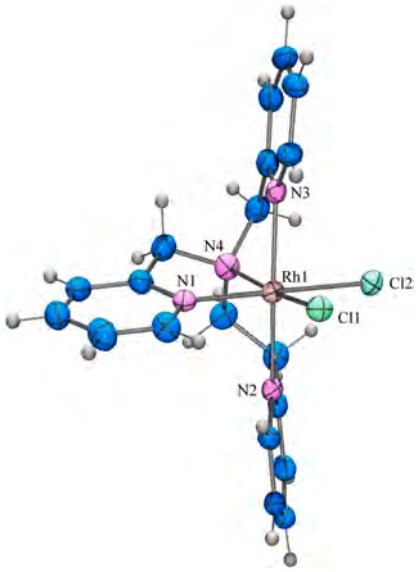

Fig. 3. Structure of one of the two independent cations in the asymmetric unit of $[Rh(pmea)Cl_2]ClO_4$ as determined by single crystal X-ray diffraction analysis. Ellipsoids are drawn at the 50% probability level. Selected bond lengths (Å) and angles (°); Rh(1)-N(1) 2.043(3), Rh(1)-N(2) 2.045(2), Rh(1)-N(3) 2.067(2), Rh(1)-N(4) 2.069(3), Rh(1)-Cl(1) 2.3554(7), Rh(1)-Cl(2) 2.3606(7); N(1)-Rh(1)-N(3) 89.48(9), N(1)-Rh(1)-N(2) 94.64(9), N(3)-Rh(1)-N(2) 172.11(10), N(1)-Rh(1)-N(4) 81.79(10), N(3)-Rh(1)-N(4) 93.28(10), N(2)-Rh(1)-N(4) 80.69(10), N(1)-Rh(1)-Cl(1) 92.49(7), N(3)-Rh(1)-Cl(1) 94.04(7), N(2)-Rh(1)-Cl(1) 92.49(7), N(4)-Rh(1)-Cl(1) 170.67(8), N(1)-Rh(1)-Cl(2) 179.31(7), N(3)-Rh(1)-Cl(2) 90.10(7), N(2)-Rh(1)-Cl(2) 85.71(7), N(4)-Rh(1)-Cl(2) 97.69(8), Cl(1)-Rh(1)-Cl(2) 88.08(3).

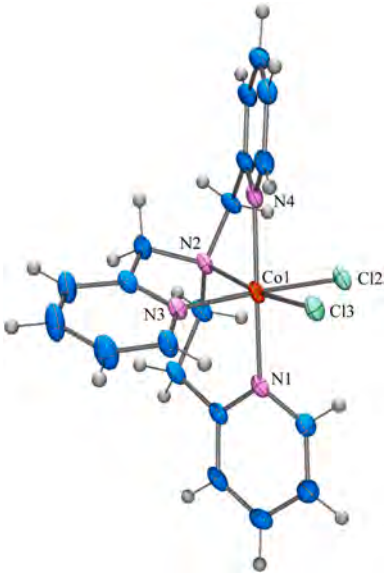

Fig. 4. Structure of the $[Co(pmea)Cl_2]^+$ cation as determined by single crystal X-ray diffraction analysis. Ellipsoids are drawn at the 50% probability level. Selected bond lengths (Å) and angles (°); Co(1)-Cl(2) 2.2412(8), Co(1)-Cl(3) 2.2599(8), Co(1)-N(1) 2.001(3), Co(1)-N(3) 1.952(3), Co(1)-N(4) 1.968(3), Co(1)-N(2) 1.979(3); Cl(2)-Co(1)-Cl3 90.36(3), N(1)-Co(1)-Cl2 87.33(7), N(1)-Co(1)-Cl(3) 93.88(8), N(3)-Co(1)-Cl(2) 176.37(8), N(3)-Co(1)-Cl3 92.07(8), N(3)-Co(1)-N(1) 89.81(10), N(3)-Co(1)-N(4) 93.28(10), N(3)-Co(1)-N2 84.59(10), N(4)-Co(1)-Cl(2) 89.40(7), N(4)-Co(1)-Cl(3) 90.33(8), N(4)-Co(1)-N(1) 174.69(11), N(4)-Co(1)-N(2) 79.57(10), N(2)-Co(1)-Cl(2) 93.49(7), N(2)-Co(1)-Cl(3) 169.13(8), N(2)-Co(1)-N(1) 96.45(10).

HSQC spectrum). However, the situation is less clear-cut for the $[Rh(pmap)Cl_2]^+$ cation; the peaks in the aliphatic region are unusually indistinct even at long acquisition times in both D_6-DMSO and D_7-DMF, and a broad peak at 57.7 ppm in the latter solvent suggested this might have been due to a fluxional process. However, the ^1H spectrum at −35 °C in D_7-DMF was essentially identical to that obtained at room temperature, arguing against this. The presence of 9 peaks in the aromatic region of the ^{13}C NMR spectrum at 25 °C is consistent with the 5-isomer (10 should be observed for this isomer, as opposed to 15 for the 6-isomer), with one peak presumably resulting from two coincident carbon atoms. The ^1H NMR of this complex in D_6-DMSO is also unexpectedly complicated, with two broad peaks in the aliphatic region at 3.59 ppm and 2.92 ppm showing no correlations in the HSQC spectrum, the geminal CH_2 doublets at 5.61 ppm and 4.70 ppm correlating to an unobserved ^{13}C signal at 72.1 ppm in the same spectrum, one proton lying under the water peak, and unusual integrations. Despite these uncertainties, the Hi-Res MS spectrum is consistent with the $[Rh(pmap)Cl_2]^+$ formulation (see above). The rigidity of the 5-membered chelate rings in the tpa, pmea, and pmap complexes is demonstrated by the observation of pairs of doublets around $\delta = 5$ ppm in their ^1H spectra, with these signals being assigned to geminal coupling of the chelate ring protons. Such signals are not observed in the more conformationally mobile tepa complex.

The X-ray crystal structure of the $[Rh(pmea)Cl_2]ClO_4$ complex confirms its formulation as the 5-isomer. This isomer was also observed in the X-ray structure of $[Rh(pmea)Cl_2]PF_6{\cdot}CH_3CN$. [39] As can be seen in Fig. 3, the structure consists of a central Rh(III) ion, coordinated to all four N atoms of a pmea ligand, and two *cis* chlorido ligands, in an approximately octahedral geometry.

The presence of a single ClO_4^- counterion confirms the 3+ oxidation state of the Rh ion, and the 5-membered chelate ring lying in the same plane as the chlorido ligands shows this to be the 5-isomer. Rh—N and Rh—Cl bond distances in the two independent cations in the asymmetric unit range from 2.027(3) Å to 2.095(3) Å, and 2.3461(8) Å to 2.3606(7) Å, respectively, similar to those found in the structure of $[Rh(pmea)Cl_2]PF_6.CH_3CN$. [39] The N-Rh-N angles in the 5-membered chelate rings are significantly smaller than those in the 6-membered rings (78.48(11)°, 80.69(10)°, 81.79(10)°, and 83.41(11)°, *versus* 93.28(10)° and 96.86(11)°, respectively), while the Cl-Rh-Cl bond angles are close to 90°. The analogous Co(III) complex $[Co(pmea)Cl_2]ClO_4$, like $[Rh(pmea)Cl_2]ClO_4$, crystallises in the $P2_1/c$ space group, but with only a single $[Co(pmea)Cl_2]^+$ cation in the asymmetric unit. The 5-isomer is again obtained (Fig. 4), albeit from a different synthetic protocol, and the smaller size of the Co(III) ion is reflected in the shorter Co—N (1.952(3) Å to 2.001(3) Å) and Co—Cl (2.2412(8) Å and 2.2599(8) Å) distances.

The N-Co-N bond angles in the 5-membered chelate rings (79.57(10)°, 84.59(10)°) are smaller than that in the 6-membered ring (96.45(10)°), and the Cl-Co-Cl angle is 90.36(3)°, slightly larger than the analogous angles in $[Rh(pmea)Cl_2]^+$ (88.08(3)° and 89.40(3)°). The most significant difference between the structures of the $[Co(pmea)Cl_2]^+$ and $[Rh(pmea)Cl_2]^+$ cations is the angle between the planes of the axial pyridine rings. In the cobalt complex the angle is 46.1°, while in the rhodium complex the angles are much smaller, at 28.8° and 20.0°. This may possibly be the result of interactions between axial parallel-displaced pyridine rings on neighbouring cations (centroid-centroid distance = 3.62 Å) in the rhodium complex that are not present in the cobalt complex.

The structure of the $[Rh(tepa)Cl_2]ClO_4$ complex (Fig. 5) shows the Rh(III) ion coordinated to all four N atoms of a tepa ligand and to two *cis*-disposed chlorido ligands in a distorted octahedral geometry. The Rh—N bonds are longer in this cation than those in the $[Rh(pmea)Cl_2]^+$ cations (average Rh—N distances are ~2.09 Å and ~ 2.06 Å, respectively), presumably as a result of the Rh(III) ion having to accommodate three 6-membered chelate rings. This is particularly evident in the Rh—N bond to the tertiary aliphatic N atom (2.122(3) Å), which is significantly longer than those in the $[Rh(pmea)Cl_2]^+$ cation (2.069(3) Å). The Rh—Cl bonds are essentially the same length in both complexes, and the

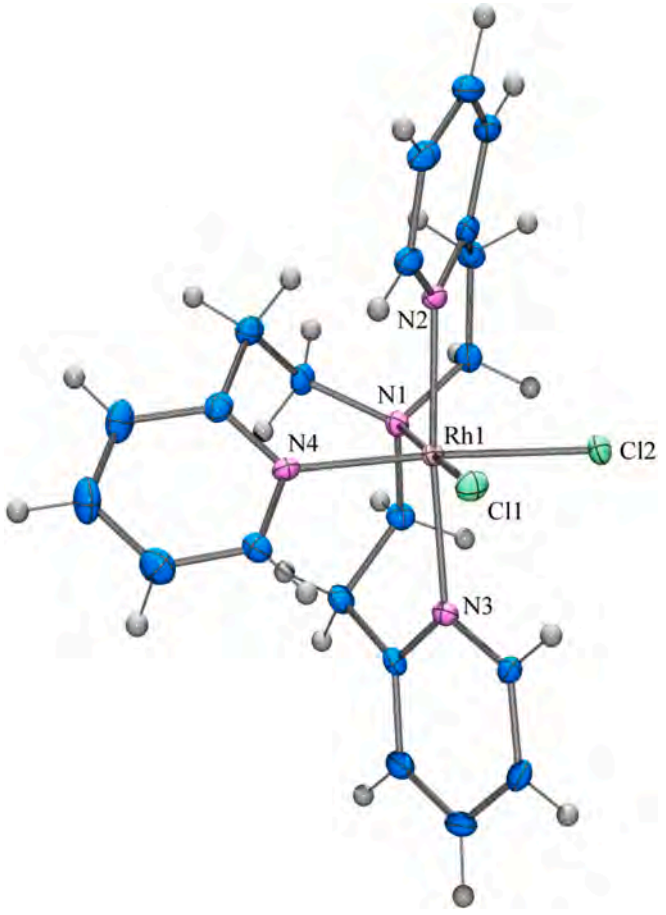

Fig. 5. Structure of the $[Rh(tepa)Cl_2]^+$ cation as determined by single crystal X-ray diffraction analysis. Ellipsoids are drawn at the 50% probability level. Selected bond lengths (Å) and angles (°); Rh(1)-N(4) 2.067(3), Rh(1)-N(2) 2.070(3), Rh(1)-N(3) 2.097(3), Rh(1)-N(1) 2.122(3), Rh(1)-Cl(2) 2.3522(8), Rh(1)-Cl(1) 2.3630(7); N(4)-Rh(1)-N(2) 93.18(10), N(4)-Rh(1)-N(3) 91.45(10), N(2)-Rh(1)-N(3) 174.07(10), N(4)-Rh(1)-N(1) 89.53(10), N(2)-Rh(1)-N(1) 89.22(10), N(3)-Rh(1)-N(1) 94.52(10), N(4)-Rh(1)-Cl(2) 175.29(7), N(2)-Rh(1)-Cl(2) 89.48(7), N(3)-Rh(1)-Cl(2) 85.66(7), N(1)-Rh(1)-Cl(2) 94.40(7), N(4)-Rh(1)-Cl(1) 89.04(8), N(2)-Rh(1)-Cl(1) 88.36(7), N(3)-Rh(1)-Cl(1) 88.02(7), N(1)-Rh(1)-Cl(1) 177.11(7), Cl(2)-Rh(1)-Cl(1) 87.15(3).

N-Rh-N bond angles in the three six-membered chelate rings are all much greater than those in the 5-membered chelate rings in $[Rh(pmea)Cl_2]ClO_4$. One of the axial pyridine rings of the tepa ligand binds noticeably bent to the Rh ion, with the Rh1-N2-C12 angle being 168.73°. A similar, but more pronounced, bending is observed in $[Co(tepa)O_2CO]ClO_4$, with the analogous angle being 163.16°. [29]

3.2. *Reactions of $[Rh(N_4)Cl_2]^+$ complexes with Na_3PO_4*

Attempts at making phosphate-containing rhodium(III) complexes involved reaction of the $[Rh(N_4)Cl_2]^+$ precursors with Na_3PO_4 in aqueous solution. Analysis of the reaction mixtures using Hi-Res MS (Figs. S6-S9) showed evidence for formation of phosphate complexes from both $[Rh(pmea)Cl_2]^+$ and $[Rh(tepa)Cl_2]^+$; $[Rh(pmea)O_2P(O)OH]^+$ (m/z = 503.0345, calculated m/z = 503.0350) was a minor product from the former, while the latter gave $[Rh(tepa)O_2P(O)OH]^+$ (m/z = 531.0657, calculated m/z = 531.0660) as the predominant product. Both cations contain a chelated hydrogenphosphate ion, which was first observed in the crystallographically characterised $[Co(pmea)O_2P(O)OH]ClO_4$ complex, [13] but which remain extremely rare. [8,14,15]. A low-intensity peak (~15%) at m/z = 266.0365 was also observed for the tepa complex. This is consistent with the 2+ cation $[Rh(tepa)O_2P(OH)OH]^{2+}$ (calculated m/z = 266.0370) which appears to contain chelated dihydrogenphosphate; there are no examples of this chelate in the CSD. Another low-intensity (~20%) peak at m/z = 495.0892 is consistent with the $[Rh(tepa)O_2CO]^+$ ion, which contains chelated carbonate (calculated m/z = 495.0900). This is presumably formed through the presence of adventitious CO_2 in the basic reaction solution. [40] No tractable phosphate-containing products were observed for the $[Rh(tpa)Cl_2]^+$ starting material, while $[Rh(pmap)Cl_2]^+$ gave the chelated carbonate complex $[Rh(pmap)O_2CO]^+$ as the base peak (m/z = 481.0739, calculated m/z = 481.0740).

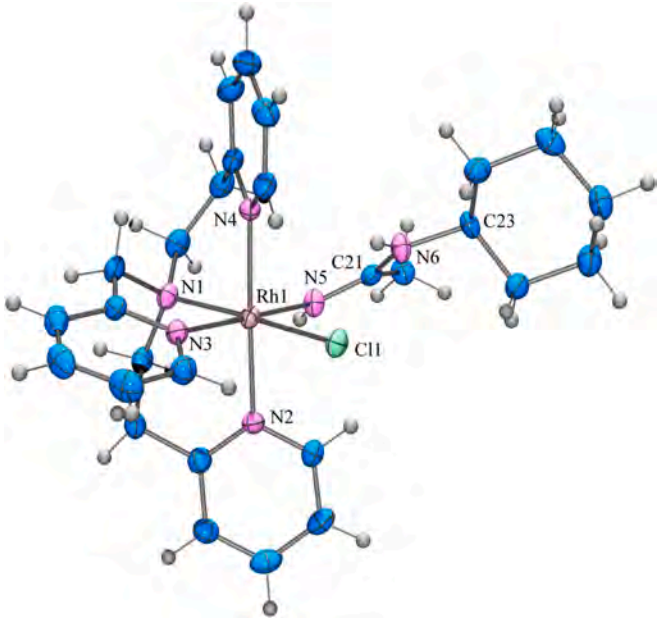

Fig. 6. Structure of the $[Rh(pmap)Cl(L)]^{2+}$ cation (L = N-cyclohexylethanimidamide) as determined by single crystal X-ray diffraction analysis. Ellipsoids are drawn at the 50% probability level. Selected bond lengths (Å) and angles (°); Rh(1)-N(5) 2.047(4), Rh(1)-N(3) 2.065(5), Rh(1)-N(4) 2.075(4), Rh(1)-N(2) 2.085(4), Rh(1)-N(1) 2.088(4), Rh(1)-Cl(1) 2.3848(11), N(5)-C(21) 1.308(6), N(6)-C(21) 1.324(6), N(6)-C(23) 1.471(6); N(5)-Rh(1)-N(3) 176.66(17), N(5)-Rh(1)-N(4) 92.49(16), N(3)-Rh(1)-N(4) 88.15(17), N(5)-Rh(1)-N(2) 84.88(18), N(3)-Rh(1)-N(2) 94.48(15), N(4)-Rh(1)-N(2) 177.37(17), N(5)-Rh(1)-N(1) 95.32(17), N(3)-Rh(1)-N(1) 81.44(17), N(4)-Rh(1)-N(1) 86.48(15), N(2)-Rh(1)-N(1) 93.88(16), N(5)-Rh(1)-Cl(1) 93.70(12), N(3)-Rh(1)-Cl(1) 89.55(12), N(4)-Rh(1)-Cl(1) 92.22(11), N(2)-Rh(1)-Cl(1) 87.83(12), N(1)-Rh(1)-Cl(1) 170.93(12), C(21)-N(5)-Rh(1) 132.1(4), N(5)-C(21)-N(6) 121.2(5), C(21)-N(6)-C(23) 126.8(4).

The nature of these products was further investigated using ^{31}P NMR spectroscopy (Figs. S10-S12). There is a paucity of 'classical' rhodium-phosphate species in the literature, and as a result, very few relevant ^{31}P NMR data are available for comparison with the complexes prepared in this work. Therefore, to aid in assignment we assume that the ^{31}P NMR chemical shifts of the Rh complexes follow those of the analogous Co(III) complexes. This appears reasonable given the similarity of the ^{13}C NMR spectra of $[Co(pmea)Cl_2]^+$ and $[Rh(pmea)Cl_2]^+$ (Figs. S19 and S21). Thus, monodentate Co(III) phosphate species generally exhibit chemical shifts between 0 and 10 ppm, and chelated species around 20–25 ppm. [24,50,51] Dimeric species with bridging phosphate ligands give larger chemical shifts (~30 ppm for bridging bidentate/monodentate and ~ 40 ppm for bridging bidentate/bidentate). The reaction mixture obtained from reaction of $[Rh(pmea)Cl_2]^+$ with Na_3PO_4 gave numerous signals between 30 and 37 ppm, which could not be easily assigned. The analogous reaction with $[Rh(pmap)Cl_2]^+$ gave almost exclusively a broad singlet at 25.1 ppm, with very minor peaks at 22.6 ppm and 21.5 ppm. The former is thought to be due to a chelated phosphate complex, while the latter could be due to small amounts of a

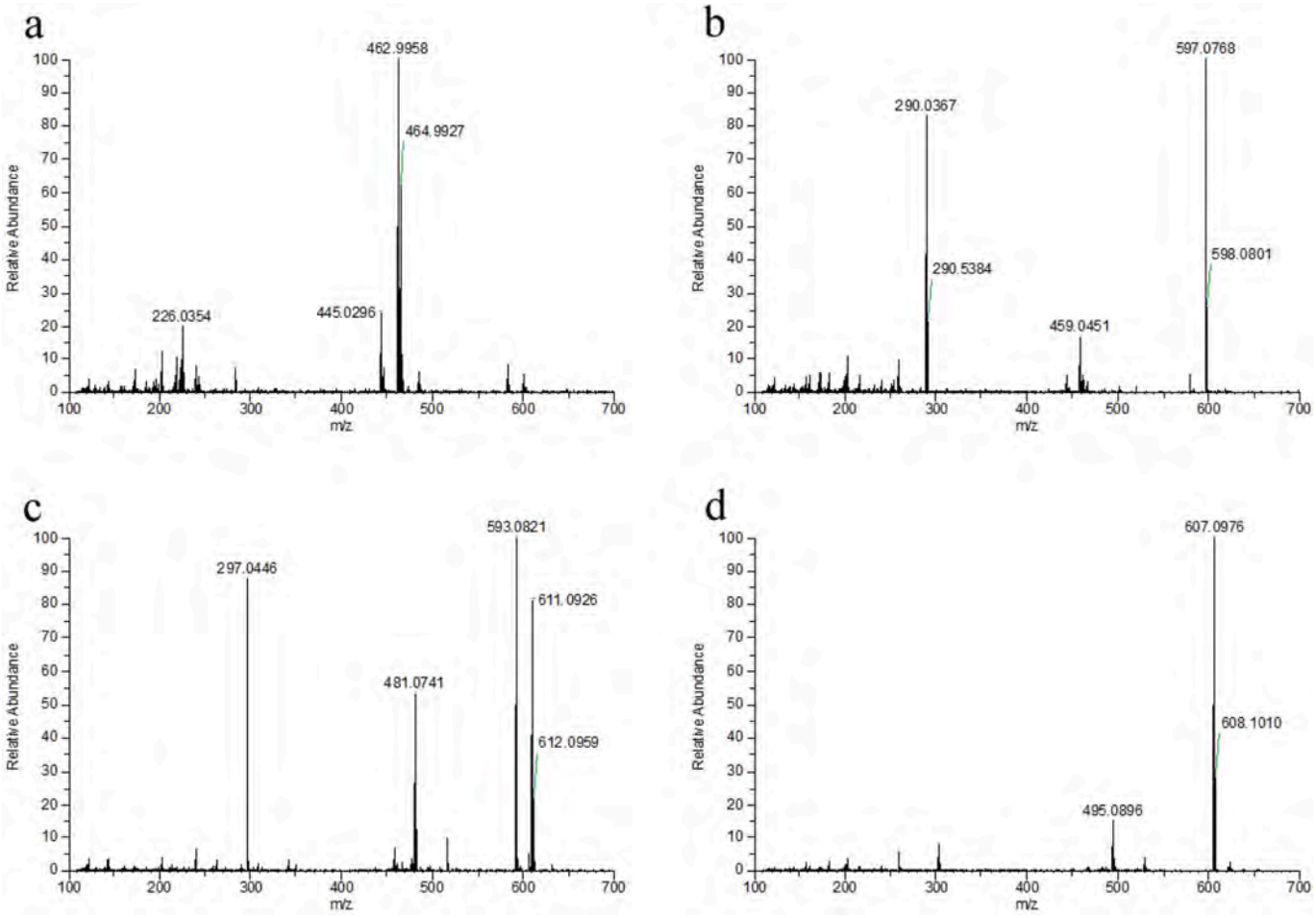

Fig. 7. Mass spectra of products obtained from reaction of a) $[Rh(tpa)Cl_2]^+$; b) $[Rh(pmea)Cl_2]^+$; c) $[Rh(pmap)Cl_2]^+$; and d) $[Rh(tepa)Cl_2]^+$ with $Na_2C_6H_5PO_4$ in aqueous solution.

5-isomer species. Most interestingly, the reaction of $[Rh(tepa)Cl_2]^+$ gave only what could be described as either a doublet or two closely spaced singlets centred at 21.0 ppm in the ^{31}P NMR spectrum, presumably arising from $[Rh(tepa)(O_2P(O)OH]^+$. As no geometric isomers are possible in this complex, it is more likely that this signal is a doublet resulting from ^{103}Rh-O-^{31}P ^2J coupling, with ^2J = 5.8 Hz. Similar coupling has been observed previously in the monodentate $[Rh(NH_3)_5OPO_3H_2]^{2+}$ ion (^2J = 1.4 Hz). [26]

3.3. Reaction of $[Rh(pmap)Cl_2]^+$ with bis(cyclohexylammonium) t-butylphosphate; the crystal structure of $[Rh(pmap)Cl(L)](ClO_4)_2$ (L = N-cyclohexylethanimidamide)

Initial attempts to prepare phosphate ester complexes of rhodium utilised bis(cyclohexylammonium)-*t*-butylphosphate. This was chosen because it was commercially available and it was thought that the *t*-butyl group might aid crystallisation from aqueous solution. The $[Rh(N_4)Cl_2]^+$ precursors were also thought to be too substitutionally inert to react with the phosphate ester and so Ag^+-induced solvolysis in acetonitrile was used to generate a more labile starting material. However, reaction of $[Rh(pmap)Cl_2]ClO_4$ with $AgCF_3SO_3$ in acetonitrile and addition of bis(cyclohexylammonium)-*t*-butylphosphate gave not the hoped-for *t*-butylphosphate complex, but the N-cyclohexylethanimidamide complex pictured in Fig. 6. The complex cation comprises a central Rh(III) ion coordinated to all four N atoms of a pmap ligand, the N atom of a monodentate N-cyclohexylethanimidamide ligand, and a chlorido ligand, which is situated *trans* to the tertiary aliphatic N atom of the pmap ligand. The 5-membered chelate ring lies in the equatorial plane, thus confirming the presence of the 5-isomer. Two ClO_4^- counterions are also present. The crystal structure confirms unexpected coordination of N-cyclohexylethanimidamide, a rare molecule, [41–43] and one which has not been previously structurally characterised, either as the free molecule or as a ligand in a complex. This appears to result from reaction of $[Rh(pmap)Cl(MeCN)]^{2+}$, formed by Ag^+-assisted solvation of $[Rh(pmap)Cl_2]^+$, with cyclohexylamine. Coordination of a nitrile to a transition metal increases the electrophilicity of the nitrile C atom through the Lewis acid effect of the metal ion, and this is known to lead to enhanced reactivity towards external nucleophiles such as OH^-, [44] CO_3^{2-}, [45] MeOH, [46] and α-phosphine carbanions. [47] Of particular relevance here are the well-known reactions of coordinated nitriles in 'classical' coordination complexes with ammonia and primary amines to give monodentate carboximidamides [48,49].

There are 27 examples of structurally characterised monodentate ethanimidamide complexes in the CSD, which have carbon-nitrogen bond lengths ranging from 1.244 Å to 1.381 Å. In all but four of these complexes, the two C—N bonds in the same molecule lie within 0.05 Å in length of each other, showing that the true bonding situation in such molecules is almost always delocalised, rather than discrete single and double amine and imine carbon nitrogen bonds. A similar situation obtains here, with the bond lengths being 1.308(6) Å and 1.324(6) Å, attesting to considerable delocalisation. The C21-N6-C23 bond angle of 126.8(4)° is also indicative of a trigonal planar, rather than pyramidal, nitrogen atom.

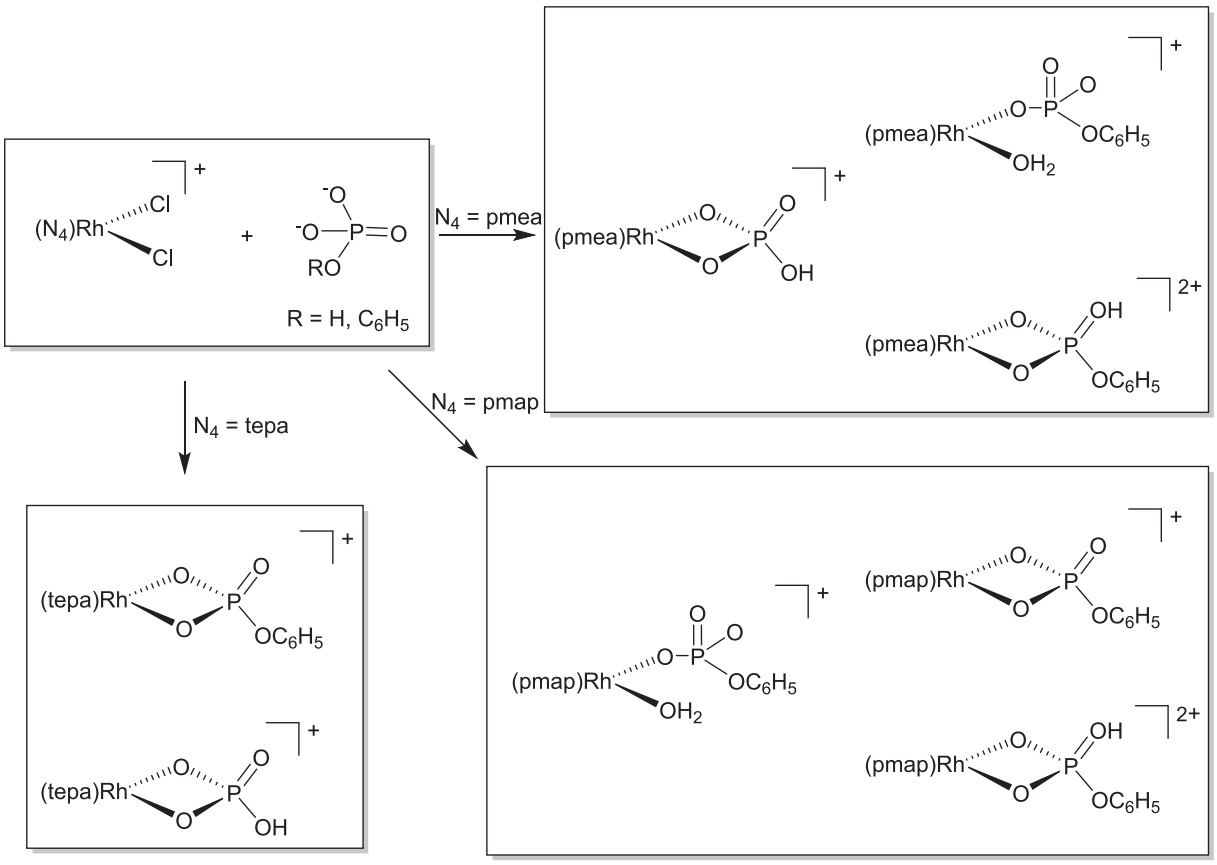

Fig. 8. Products identified from the reaction of $[Rh(N_4)Cl_2]^+$ with Na_3PO_4 and $Na_2C_6H_5PO_4$.

3.4. Reactions of $[Rh(N_4)Cl_2]^+$ complexes with disodium phenylphosphate; product identification by mass spectrometry

Given the interference caused by the cyclohexylammonium counterion described above, further attempts to prepare phosphate ester complexes utilised disodium phenylphosphate $Na_2C_6H_5PO_4$ as the phosphate ester source. Reaction of this with the $[Rh(N_4)Cl_2]ClO_4$ precursors in water in the presence of a variety of counteranions gave no crystalline materials. However, analysis of the reaction mixtures with Hi-Res MS gave evidence for the formation of phosphate ester species in solution for all but the tpa complex, which remained essentially unchanged under these reaction conditions (Fig. 7), and the products of these reactions, plus those from the reactions with Na_3PO_4, are summarised in Fig. 8.

Reaction of $[Rh(pmea)Cl_2]^+$ with $Na_2C_6H_5PO_4$ resulted in a base peak at $m/z = 597.0768$ and a slightly less intense (~85%) peak at $m/z = 290.0367$. The former is consistent with the formula $[Rh(pmea)(O_2P(O)OC_6H_5)(OH_2)]^+$, which could be a complex containing a monodentate phosphate ester and an aqua ligand. The latter peak, most interestingly, is consistent with the formula $[Rh(pmea)(O_2P(OH)OC_6H_5]^{2+}$, containing a protonated, chelated phosphate ester ligand. Using $[Rh(pmap)Cl_2]^+$ as a starting material gives a reaction mixture which similarly appears to contain the monodentate phosphate ester complex $[Rh(pmap)(O_2P(O)OC_6H_5)(OH_2)]^+$ ($m/z = 611.0930$) and the protonated, chelated phosphate ester complex $[Rh(pmap)(O_2P(OH)OC_6H_5]^{2+}$ ($m/z = 297.0446$). In addition, the base peak at $m/z = 593.0821$ is consistent with the formula $[Rh(pmap)(O_2P(O)OC_6H_5]^+$, the non-protonated chelated phosphate ester complex. A less intense peak at $m/z = 481.0741$ can be ascribed to the $[Rh(pmap)O_2CO]^+$ complex, presumably formed from the presence of adventitious CO_2 in the basic reaction mixture.

The trend is continued when $[Rh(tepa)Cl_2]^+$ is used as the starting material. In this case, the reaction mixture shows a predominant single Hi-Res MS peak at $m/z = 607.0976$, which corresponds to the chelated phosphate ester complex $[Rh(tepa)(O_2P(O)OC_6H_5]^+$, with the only other peak of note (~20%) being due to $[Rh(tepa)O_2CO]^+$ ($m/z = 495.0896$).

The reactions with $Na_2PO_4C_6H_5$ appear similar to those with Na_3PO_4 in terms of the ^{31}P NMR spectra obtained (Figs. S13–15). The reactions with both $[Rh(pmea)Cl_2]^+$ and $[Rh(pmap)Cl_2]^+$ give numerous peaks, none of which can be assigned with certainty, but which appear to be mostly monodentate species. Both complexes, however, exhibit peaks around 25 ppm, which can be assigned to either the chelated phosphate ester or chelated phosphate complex. The mass spectral data are consistent with the former. The ^{31}P spectrum obtained from reaction of the $[Rh(tepa)Cl_2]^+$ is simpler, with peaks due to free ester (−3.7 ppm) and an unidentified species (14.3 ppm, base peak) observed. In addition, a doublet at 21.5 ppm ($^2J = 5.1$ Hz), which can be assigned to either a chelated phosphate ester, or chelated phosphate complex, is observed. Again, the mass spectral data are consistent with the former.

The combined mass spectral and NMR evidence are therefore consistent with the formation of chelated phosphate ester complexes in solution. While in no cases are they the dominant species, the fact that they are stable under mass spectrometry and NMR conditions suggests that isolation following chromatography may well be possible.

4. Conclusions

The reaction of substitutionally inert Rh(III) complexes with both phosphate and phenylphosphate in aqueous solution gives a variety of phosphorus-containing species. It appears that the presence of one or more 6-membered chelate rings in the ancillary N_4 ligand facilitates the formation of chelated phosphate species. Of these, the observation of unprecedented stable chelated phosphate esters is particularly

interesting, and suggests they are amenable to isolation and characterisation.

CRediT authorship contribution statement

Ruojie Huang: Investigation. **Cameron P. Waghorn:** Investigation. **Timothy D. Christopher:** Investigation, Formal analysis. **Tilo Söhnel:** Investigation, Formal analysis. **Tony Chen:** Formal analysis. **Allan G. Blackman:** Writing – review & editing, Writing – original draft, Supervision, Investigation, Conceptualization.

Funding sources

This research did not receive any specific grant from funding agencies in the public, commercial, or not-for-profit sectors.

Declaration of competing interest

The authors declare that they have no known competing financial interests or personal relationships that could have appeared to influence the work reported in this paper.

Appendix A. Supplementary data

Supplementary data to this article can be found online at https://doi.org/10.1016/j.poly.2026.118300.

Data availability

Data will be made available on request.

References

[1] D. Gani, J. Wilkie, Metal ions in the mechanism of enzyme-catalysed phosphate monoester hydrolyses, in: H.A.O. Hill, P.J. Sadler, A.J. Thomson (Eds.), Metal Sites in Proteins and Models: Phosphatases, Lewis Acids and Vanadium, Springer Berlin Heidelberg, Berlin, Heidelberg, 1997, pp. 133–175, https://doi.org/10.1007/3-540-62874-6_11.

[2] K.L. Haas, K.J. Franz, Application of metal coordination chemistry to explore and manipulate cell biology, Chem. Rev. 109 (2009) 4921–4960, https://doi.org/10.1021/cr900134a.

[3] C. Liu, L. Wang, DNA hydrolytic cleavage catalyzed by synthetic multinuclear metallonucleases, Dalton Trans. (2009) 227–239, https://doi.org/10.1039/B811616D.

[4] C. Liu, M. Wang, T. Zhang, H. Sun, DNA hydrolysis promoted by di- and multinuclear metal complexes, Coord. Chem. Rev. 248 (2004) 147–168, https://doi.org/10.1016/j.cct.2003.11.002.

[5] P. Hendry, A.M. Sargeson, Metal ion promoted reactions of phosphate derivatives, Prog. Inorg. Chem. 38 (1990) 201.

[6] M.D. Tomczyk, N. Kuźnik, K. Walczak, Cyclen-based artificial nucleases: three decades of development (1989–2022). Part A – hydrolysis of phosphate esters, Coord. Chem. Rev. 481 (2023) 215047, https://doi.org/10.1016/j.ccr.2023.215047.

[7] H.-B. Luo, X.-R. Wu, X.-W. Li, Z. Zhang, K.-X. Zhao, F.-R. Lin, G.-Q. Zhang, X.-S. Gao, Y. Liu, X.-M. Ren, Alginate beads embedded with metal-organic framework particles for solid-phase detoxification of organophosphate under ambient conditions, Inorg. Chem. 65 (2026) 709–715, https://doi.org/10.1021/acs.inorgchem.5c04951.

[8] Z.N. Gafurov, A.B. Dobrynin, I.F. Sakhapov, A.A. Kagilev, A.O. Kantyukov, A. A. Balabaev, A.V. Toropchina, O.G. Sinyashin, D.G. Yakhvarov, New 2,2′-bipyridine and 1,10-phenanthroline based nickel(II) phosphates, Phosphorus Sulfur Silicon Relat. Elem. 194 (2019) 517–521, https://doi.org/10.1080/10426507.2018.1541243.

[9] B. Anderson, R.M. Milburn, J.M. Harrowfield, G.B. Robertson, A.M. Sargeson, Cobalt(III)-promoted hydrolysis of a phosphate ester, J. Am. Chem. Soc. 99 (1977) 2652–2661, https://doi.org/10.1021/ja00450a042.

[10] A.S. Kumbhar, M.S. Deshpande, R.J. Butcher, Hydrogen bond directed open-framework of bis(bipyridine-glycoluril) phosphatocobalt(III) with solvent accessible void space, CrystEngComm 10 (2008) 1520–1523, https://doi.org/10.1039/b806123h.

[11] E. Rojas-Gatjens, C. Viales-Montero, R. Urcuyo, D. González-Flores, M.L. Montero, Oxidative dissolution of synthetic vivianites as a method for the crystallization of molecular structural motifs, Struct. Chem. 32 (2021) 445–455, https://doi.org/10.1007/s11224-020-01644-3.

[12] Y. Funahashi, A. Yoneda, C. Taki, M. Kosuge, T. Ozawa, K. Jitsukawa, Hideki. Masuda, Novel phosphate-phosphate bond formation mediated upon cobalt (III) complex systems, Chem. Lett. 34 (2005) 1332–1333, https://doi.org/10.1246/cl.2005.1332.

[13] L.F. McClintock, A.G. Blackman, A structural model for HPO_4^{2-} binding to Co in a water oxidation catalyst, Chem. Asian J. 5 (2010) 756–758, https://doi.org/10.1002/asia.200900728.

[14] S.-Y. Chen, Y.-C. Guo, L.-F. Zhang, Y.-Q. Feng, Y.-Y. Zhang, Jiegou Huaxue (Chin.J. Struct.Chem.) 32 (2013) 643.

[15] D.-F. Qiu, Y.-C. Guo, Y.-Q. Feng, S.-Y. Chen, M.-Z. Sai, Hydrothermal syntheses, crystal structures and photoluminescence property of complexes, Wuji Huaxue Xuebao 26 (2010) 1663–1668.

[16] D. Desbouis, I.P. Troitsky, M.J. Belousoff, L. Spiccia, B. Graham, Copper(II), zinc(II) and nickel(II) complexes as nuclease mimetics, Coord. Chem. Rev. 256 (2012) 897–937, https://doi.org/10.1016/j.ccr.2011.12.005.

[17] D. Andrew Knight, J.B. Delehanty, E.R. Goldman, J. Bongard, F. Streich, L. W. Edwards, E.L. Chang, Carboxylic acid functionalized cobalt(III) cyclen complexes for catalytic hydrolysis of phosphodiester bonds, Dalton Trans. (2004) 2006–2011, https://doi.org/10.1039/B405307A.

[18] J. Chin, M. Banaszczyk, V. Jubian, Xiang. Zou, Cobalt(III) complex-promoted hydrolysis of phosphate diesters: comparison in reactivity of rigid cis-diaquo (tetraaza)cobalt(III) complexes, J. Am. Chem. Soc. 111 (1989) 186–190, https://doi.org/10.1021/ja00183a029.

[19] R. Hettich, H.-J. Schneider, Cobalt(III) polyamine complexes as catalysts for the hydrolysis of phosphate esters and of DNA. A measurable 10 million-fold rate increase, J. Am. Chem. Soc. 119 (1997) 5638–5647, https://doi.org/10.1021/ja964319o.

[20] R.D. Wijesekera, A.M. Sargeson, Reactivities of coordinated phosphodiesters, J. Coord. Chem. 58 (2005) 3–19, https://doi.org/10.1080/00958970512331327393.

[21] M. Padovani, N.H. Williams, P. Wyman, Mononuclear co(III)-complex promoted phosphate diester hydrolysis: dependence of reactivity on the leaving group, J. Phys. Org. Chem. 17 (2004) 472–477, https://doi.org/10.1002/poc.770.

[22] R.L. Fanshawe, A.G. Blackman, C.R. Clark, The hydrolysis of 4-nitrophenylphosphate promoted by $[(N)_4Co(OH/H)(OH/H)]^{+/2+/3+}$ species ($(N)_4$=abap, tren); use of ^{31}P NMR to uncover mechanistic complexity, Inorg. Chim. Acta 342 (2003) 114–124, https://doi.org/10.1016/S0020-1693(02)01170-2.

[23] D. Wahnon, A.-M. Lebuis, J. Chin, Hydrolysis of a phosphate diester doubly coordinated to a dinuclear cobalt(III) complex: a novel mechanism, Angew. Chem. Int. Ed. Engl. 34 (1995) 2412–2414, https://doi.org/10.1002/anie.199524121.

[24] F. Seel, G. Bohnstedt, Phosphorus-31 NMR spectroscopic investigations of phosphato complexes of cobalt(III) and rhodium(III), Z. Anorg. Allg. Chem. 435 (1977) 257–267.

[25] M. Martinez, M. Ferrer, Synthesis of pentaammine(phosphato)rhodium(III) and kinetics of formation of its diprotonated form, Inorg. Chem. 24 (1985) 792, https://doi.org/10.1021/ic00199a033.

[26] A.V. Belyaev, S.V. Tkachev, Complexation of the $[Rh(NH_3)_5H_2O]^{3+}$ ion in aqueous solutions of H_3PO_4 based on ^{31}P NMR data, Russ. J. Coord. Chem. 38 (2012) 445–449, https://doi.org/10.1134/s1070328412060024.

[27] M.A. Fedotov, A.V. Belyaev, The first (^{31}P, ^{17}O, and ^{103}Rh) NMR observation complex formation of rhodium(III) with phosphoric acid, Russ. J. Inorg. Chem. 53 (2008) 761–764, https://doi.org/10.1134/S0036023608050148.

[28] A.V. Belyaev, S.N. Vorob'eva, M.A. Fedotov, ^{103}Rh, ^{17}O, and ^{31}P NMR study of Rh (III) complex formation in acidic sulfate-phosphate media, Russ. J. Inorg. Chem. 57 (2012) 231–236, https://doi.org/10.1134/S0036023612020040.

[29] P.M. Jaffray, L.F. McClintock, K.E. Baxter, A.G. Blackman, Cobalt(III) carbonate and bicarbonate chelate complexes of tripodal tetraamine ligands containing pyridyl donors: the steric basis for the stability of chelated bicarbonate complexes, Inorg. Chem. 44 (2005) 4215–4225, https://doi.org/10.1021/ic0482537.

[30] S.E. Cheyne, L.F. McClintock, A.G. Blackman, Stabilization of coordinated carbonate in aqueous acidic solution: steric inhibition of protonation in Co(III) complexes containing chelated carbonate, Inorg. Chem. 45 (2006) 2610–2618, https://doi.org/10.1021/ic0521325.

[31] J. Yang, E.M. Leitao, M.A. Nascimento, T.D. Christopher, T. Söhnel, T. Chen, L. R. Gahan, A.G. Blackman, Werner complexes can still surprise: the chelated O_2BOH^{2-} ligand, Inorg. Chem. 64 (2025) 13415–13421, https://doi.org/10.1021/acs.inorgchem.5c01904.

[32] M. Schatz, M. Becker, F. Thaler, F. Hampel, S. Schindler, R.R. Jacobson, Z. Tyeklar, N.N. Murthy, P. Ghosh, Q. Chen, J. Zubieta, K.D. Karlin, Copper(I) complexes, copper(I)/O_2 reactivity, and copper(II) complex adducts, with a series of tetradentate tripyridylalkylamine tripodal ligands, Inorg. Chem. 40 (2001) 2312–2322.

[33] G. Anderegg, F. Wenk, Pyridine derivatives as complexing agents. VIII. Preparation of a new quadridentate and a new hexadentate ligand, Helv. Chim. Acta 50 (1967) 2330–2332.

[34] G.M. Sheldrick, A short history of SHELX, Acta Crystallogr. Sect. A: Found. Crystallogr. 64 (2008) 112–122, https://doi.org/10.1107/S0108767307043930.

[35] M.C. Burla, R. Caliandro, B. Carrozzini, G.L. Cascarano, C. Cuocci, C. Giacovazzo, M. Mallamo, A. Mazzone, G. Polidori, Crystal structure determination and refinement via SIR2014, J. Appl. Cryst. 48 (2015) 306–309, https://doi.org/10.1107/S1600576715001132.

[36] G.M. Sheldrick, Crystal structure refinement with SHELXL, Acta Crystallogr. C 71 (2015) 3–8, https://doi.org/10.1107/S2053229614024218.

[37] L.J. Farrugia, WinGX suite for small-molecule single-crystal crystallography, J. Appl. Cryst. 32 (1999) 837–838, https://doi.org/10.1107/S0021889899006020.

[38] O.V. Dolomanov, L.J. Bourhis, R.J. Gildea, J.A.K. Howard, Horst. Puschmann, OLEX2: a complete structure solution, refinement and analysis program, J. Appl. Crystallogr. 42 (2009) 339–341, https://doi.org/10.1107/S0021889808042726.

[39] D.G. Lonnon, D.C. Craig, S.B. Colbran, Rhodium, palladium and platinum complexes of tris(pyridylalkyl)amine and tris(benzimidazolylmethyl)amine N_4-tripodal ligands, Dalton Trans. (2006) 3785–3797, https://doi.org/10.1039/b602556k.
[40] F. Ismael, C.L. Fleming, L.R. Gahan, A.G. Blackman, Chelated O_2BOH^{2-} or chelated O_2CO^{2-}: an isoelectronic conundrum, Inorg. Chem. 62 (2023) 18025–18028, https://doi.org/10.1021/acs.inorgchem.3c03149.
[41] L. Baiocchi, G. Palazzo, Reactions of imidates. Preparation of amidines and N-substituted imidates, Ann. Chim. 58 (1968) 608.
[42] W.A. Bolhofer, C.N. Habecker, A.M. Pietruszkiewicz, M.L. Torchiana, H.I. Jacoby, C.A. Stone, 2-Mercaptoacetamidines as gastric antisecretory agents, J. Med. Chem. 22 (1979) 295–301, https://doi.org/10.1021/jm00189a015.
[43] S. Tollari, F. Porta, Stoichiometric and catalytic oxidation of cyclohexylamine by $Mo(O)(O_2)_2(H_2O)$(HMPA), J. Mol. Catal. 84 (1993) L137, https://doi.org/10.1016/0304-5102(93)85045-u.
[44] D.A. Buckingham, F.R. Keene, A.M. Sargeson, Base hydrolysis of coordinated acetonitrile, J. Am. Chem. Soc. 95 (1973) 5649–5652, https://doi.org/10.1021/ja00798a032.
[45] I.I. Creaser, J.M.B. Harrowfield, F.R. Keene, A.M. Sargeson, Reactivity of coordinated nitriles, J. Am. Chem. Soc. 103 (1981) 3559–3564, https://doi.org/10.1021/ja00402a051.
[46] F.P. Fanizzi, F.P. Intini, G. Natile, Nucleophilic attack of methanol on bis(benzonitrile)dichloroplatinum: formation of mono- and bis-imido ester derivatives, J. Chem. Soc. Dalton Trans. (1989) 947–951, https://doi.org/10.1039/DT9890000947.
[47] P. Braunstein, D. Matt, Y. Dusausoy, J. Protas, Reaction of α-phosphino functional carbanions with co-ordinated nitriles. Synthesis of bis-chelate (P,N) platinum complexes; X-ray crystal and molecular structure of trans-$Pt[P(Ph)_2C(CO_2Et)C(Ph)NH]_2$, J. Chem. Soc. Chem. Commun. (1979) 763–764, https://doi.org/10.1039/C39790000763.
[48] D.P. Fairlie, W.G. Jackson, Amination of coordinated nitriles: synthesis of metal complexes of amidines and guanidines, Inorg. Chem. 29 (1990) 140–143, https://doi.org/10.1021/ic00326a030.
[49] V.Yu. Kukushkin, A.J.L. Pombeiro, Additions to metal-activated organonitriles, Chem. Rev. 102 (2002) 1771–1802, https://doi.org/10.1021/cr0103266.
[50] G.P. Haight, T.W. Hambley, P. Hendry, G.A. Lawrance, A.M. Sargeson, Rapid cleavage of tridentate cobalt(III)-co-ordinated triphosphate, J. Chem. Soc. Chem. Commun. (1985) 488–491, https://doi.org/10.1039/C39850000488.
[51] G.P. Haight, Hydrolysis of phosphate esters and anhydrides: role of metal ions, Coord. Chem. Rev. 79 (1987) 293–319, https://doi.org/10.1016/0010-8545(87)80008-5.